Femtosecond-Laser Assisted Surgery of Eye

Fs-laser technology is unique because it allows cutting tissue at very high precision inside the eye. Fs lasers are mainly used for surgery of the human cornea and lens. New areas of application in ophthalmology are on the horizon. The latest improvement is the high pulse frequency, low-energy concept; by enlarging the numerical aperture of the focusing optics, the pulse energy threshold for optical breakdown decreases, and cutting with practically no side effects is enabled.

1. Introduction

Laser technology and ophthalmic surgery have shaped each other over the past 40 years. The optically transparent structures of the eye, namely cornea, lens, and vitreous body, allow for delivery of the laser energy at different focal depths, thereby giving access to surgical interventions without having to open or mechanically enter the eye (Figure 1). Other types of lasers, with various wavelengths, pulse durations, and power levels, interact with eye tissues in a range of different ways. For continuous laser irradiation of low to moderate average power (mW range), photochemical and thermal effects induced by the absorbed light are the dominant laser–tissue interactions. Depending on the wavelengths used, specific types of molecules can be optically excited to trigger chemical reactions, or local heating of specific tissue can be achieved. If temperatures above 60 °C are reached, tissue coagulation will occur. When pulsed laser light with intensities between 10^7 and 10^9 W/cm^2 interacts with strongly absorbing tissue, near-surface material can be removed explosively. This effect is called "photoablation". In ophthalmology, it is applied to change the curvature of the cornea with pulsed UV light from excimer lasers. For shorter pulse durations in the ps to fs range and even higher intensities above 10^{11} W/cm^2, more exotic interactions can be achieved, as will be explained in detail below. A more comprehensive general overview of laser–tissue interaction mechanisms can be found in excellent quality in several text books [1][2].

The first reported ophthalmic use of short pulse lasers at near-infrared wavelengths was in 1979 by Aron-Rosa, who treated posterior capsule opacification (PCO) after cataract surgery [3]. In 1989, Stern et al. demonstrated that by decreasing pulse width of ultrashort-pulsed lasers from nano- to femtoseconds (ns: 10^{-9} s, fs: 10^{-15} s), ablation profiles showed higher precision and less collateral damage [4]. At the same time, optical coherence tomography developed and provided noninvasive three-dimensional (3D) in vivo imaging with fine resolution in both lateral and axial dimensions at a micrometer level [5]. These developments offered ophthalmic surgeons a tool for high precision cutting and visual control through imaging, and ultimately allowed a gamut of treatment applications for these lasers within the field of ophthalmology. Recent changes in the numerical aperture of the laser focusing optics and the repetition rate of the laser sources have further decreased collateral damage while increasing precision.
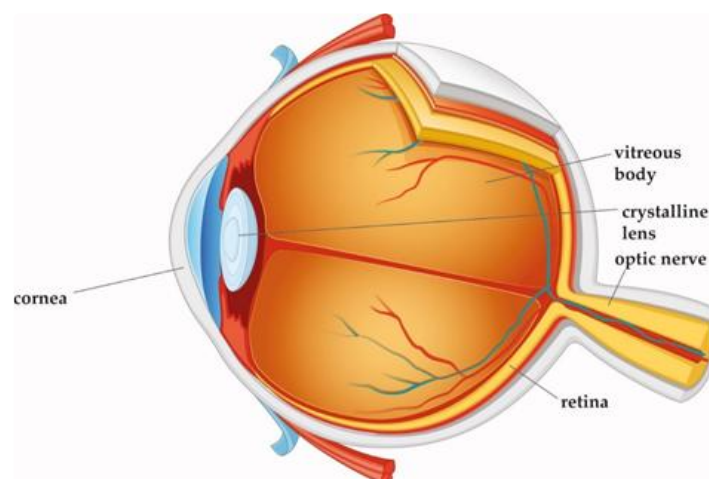

Figure 1. Cross-section of the eye. Cornea, crystalline lens, and vitreous body are transparent in the healthy eye.

2. Laser Technology

2.1. Solid-State Lasers in Ophthalmology

2.1.1. Nd:YAG Laser with Ns Pulse Durations

The first type of short-pulsed laser at near-infrared wavelengths successfully used in ophthalmology was the Q-switched Nd:YAG solid-state laser. Its wavelength of 1064 nm is transmitted by all the visually transparent structures in the eye (cornea, lens, and vitreous body). Their pulse durations are a few nanoseconds (ns), and for ophthalmic applications, pulse energies in the range of 0.3–10 mJ are typically used [6].

When Nd:YAG laser pulses are strongly focused at a location inside the eye, to spot sizes in the order of a few microns, the combination of short pulse duration focusing to minimal spot sizes creates very high intensities at the laser focus, above 10^{11} W/cm^2. Under these conditions, a phenomenon called "optical breakdown" occurs. In the first step, multiphoton absorption leads to ionization of some tissue molecules, creating free electrons. In the subsequent second step, these "seed" electrons absorb photon energy and are thus accelerated. After repeated photon absorptions, electrons reach a sufficiently high kinetic energy to ionize themselves more molecules by impact ionization, creating more free electrons. If the laser irradiation is intense enough to overcome electron losses, an avalanche effect occurs [2].

When the extremely fast rising electron density exceeds values of approximately 10^{20}/cm^3, a "plasma state of matter" (cloud of ions and free electrons) is created at the laser focus [2]. This plasma is highly absorbing for photons of all wavelengths. Therefore, the rest of the laser pulse is directly absorbed by the plasma, increasing its temperature and energy density (Figure 2).

The hot plasma cloud rapidly recombines to a hot gas, with a thermalization time of the energy initially carried by free electrons of a few picoseconds to tens of ps [7]. This time is much shorter than the acoustic transit time from the center of the focus to the periphery of the plasma volume, leading to confinement of the thermoelastic stresses caused by the temperature rise. Conservation of momentum requires that the stress wave emitted in this geometrical configuration contains both compressive and tensile components [7]. If sufficient pulse energy density is applied, the tensile stress wave becomes strong enough to induce fracture of the tissue, causing the formation of a cavitation bubble [7]. Depending on the pulse energy, the pressure wave can reach supersonic speed a (shock wave). The high plasma temperature also leads to almost immediate evaporation of the tissue within the focal volume, generating water vapor and gases such as H_2, O_2, methane, and ethane [8]. The resulting gas pressure pushes the surrounding tissue further away, adding to the expansion of the short-lived bubble inside the tissue (Figure 2). The maximum volume temporarily achieved by the bubble scales with the pulse energy above the threshold for optical breakdown. During bubble expansion, the inside pressure ultimately drops below atmospheric pressure due to the outward moving material's inertia, resulting in the bubble dynamically collapsing. The bubble collapse may create another shock wave [2]. This combined process is called "photodisruption" of tissue.
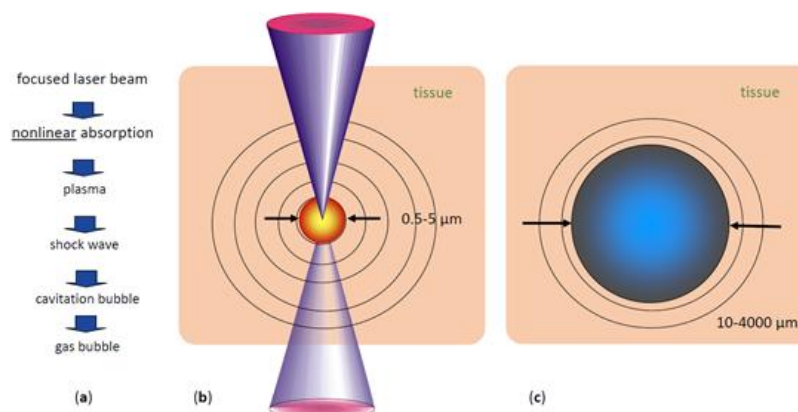

Figure 2. Short pulse laser effects in tissue: (**a**) sequence of effects and induced events, (**b**) plasma size range and pressure wave pattern, (**c**) range of possible cavitation bubble dimensions (pulse energy-dependent) [9].

With typical ophthalmic Nd:YAG laser pulse energies, cavitation bubble radii are in the range of 1000–2000 μm, and shock wave amplitudes at 1 mm distance from the focus reach 100–500 bar [10]. These rather pronounced mechanical side effects restrict the use of Nd:YAG lasers. When shorter pulse ps (10^{-12} s) lasers became available, their mechanical side effects proved to be still too large for delicate tasks as required for ophthalmic applications. This limits Nd:Yag laser application in today's clinical ophthalmological use to cutting isolated tissues, such as the lens capsule in posterior capsular opacification in pseudophakes or small areas of iris tissue to improve aqueous dynamics within the eye.

2.1.2. Femtosecond Lasers

Femtosecond lasers are a more recent advance in solid-state laser technology. They operate at near-infrared wavelengths similar to Nd:YAG lasers but at pulse durations of less than 1 picosecond (ps). As the threshold radiant exposure (J/cm^2) for inducing optical breakdown in tissue is about two orders of magnitude lower in the fs pulse duration regime than at 10 ns [11], much lower pulse energies can be applied to separate tissue. High pulse repetition rates from 10 s of kHz to even MHz are then used to create continuous cut planes inside the tissue by placing many pulses close to each other with three-dimensional beam scanning systems.

The lower pulse energies lead to a drastic reduction of the mechanical side effects of optical breakdown. For 300 fs pulses of 0.75 µJ energy, the generated cavitation bubbles have radii of only 45 µm, almost two orders of magnitude smaller than ns pulse with energies in the mJ range [12]. In addition, the associated pressure waves are much weaker, 1–5 bar at 1 mm distance [13]. This process is referred to as "plasma-induced ablation", as the disruptive mechanical side effects of ns pulses described above are absent. Additionally, the thermal side effects of fs pulses in tissue are almost negligible [7].

The first commercially available, USA Food and Drug Administration (FDA)-approved fs-laser system for ophthalmology, the IntraLase^{TM} FS, was launched in 2001 [14]. It was used for "flap" creation in LASIK refractive surgery (see Section 3.1.1 below), replacing mechanical cutting devices called microkeratomes. Its first commercial version operated at a 15 kHz repetition rate and pulse energies of several µJ [15]. Further fs-laser systems for "flap" cutting and other corneal surgery were launched by several manufacturers in the following years, including the Ziemer FEMTO LDV in 2005, which introduced a new concept of low pulse energies and high repetition rates, and later the Wavelight FS200 and the Zeiss VisuMax^{TM}.

In 2009, the LensX^{TM} system was introduced, the first commercial fs laser designed for cataract surgery, thus opening a new field of fs-laser application within ophthalmology [16]. Its early versions operated at 33 kHz repetition rate and pulse energies of 6–15 µJ [17]. LensX became part of Alcon, and again, in the following years, multiple other manufacturers launched similar products, including the Johnson & Johnson Optimedica Catalys^{TM}, the LENSAR® and the Bausch and Lomb Victus^{TM}.

2.1.3. Modern Low Pulse Energy High Repetition Rate Fs Lasers

The pulse energy required to achieve optical breakdown can be reduced in two ways:

First, by shortening the pulse duration—the latest fs lasers can achieve pulse durations of 200–300 fs, while earlier models had pulse durations of up to 800 fs.

Second, by reducing the focal spot size—the focal volume of a Gaussian laser beam is dependent on the axial extension, the so-called Rayleigh range ($z_R = \pi w_0^2/\lambda$) and the beam waist $w_0 = f\lambda/\pi w_L$, where f is the focal length of the lens, w_0 the beam radius at the focus, and w_L the beam radius at the focusing lens. In other words, the focal volume varies inversely with the cube of the numerical aperture NA = w_L/f of the focusing optics (Figure 3). The larger the numerical aperture NA, the smaller the focal spot and finally, the smaller the energy threshold for optical breakdown [18].
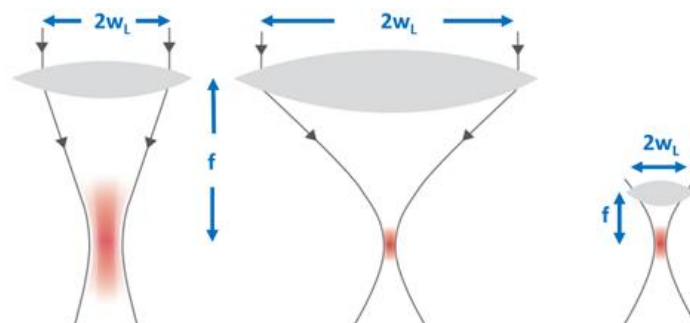

Figure 3. The focal volume of a Gaussian laser beam scales with the numerical aperture NA = w/f of the focusing lens. The larger the NA, the smaller the focal spot volume.

To practically achieve high NA focusing optics, either the lens diameter can be increased, which quickly becomes bulky and expensive, or the focusing optics can be positioned closer to the eye. The latter approach was implemented by Ziemer Ophthalmic Systems, using a microscope lens with a short focal length as focusing optics and guiding the laser beam via an articulated mirror arm to a handpiece containing the focusing optics, which is docked to the eye at a short distance.

In 2014, the first low pulse energy fs-laser system for cataract and cornea surgery, the Ziemer FEMTO LDV Z8^{TM}, was CE-approved and commercially launched. It was more compact and lightweight than its predecessors, enabling mobile use.

2.2. Femtosecond Laser–Tissue Interaction

Based on the above laser parameters, the nature of the cutting processes of the two groups differs. In the high pulse energy laser group, the cutting process is driven by mechanical forces applied by the expanding bubbles. The bubbles disrupt the tissue at a larger radius than the plasma created at the laser focus (Figure 4a). On the other hand, in the low pulse energy group, spot separations smaller than the spot sizes are used for overlapping plasmas, which directly evaporate the tissue inside the plasma volume, effectively separating tissue without a need for secondary mechanical tearing effects (Figure 4b). Due to the high pulse repetition rates applied (MHz range), the cutting speeds achieved are similar to the high energy laser group.
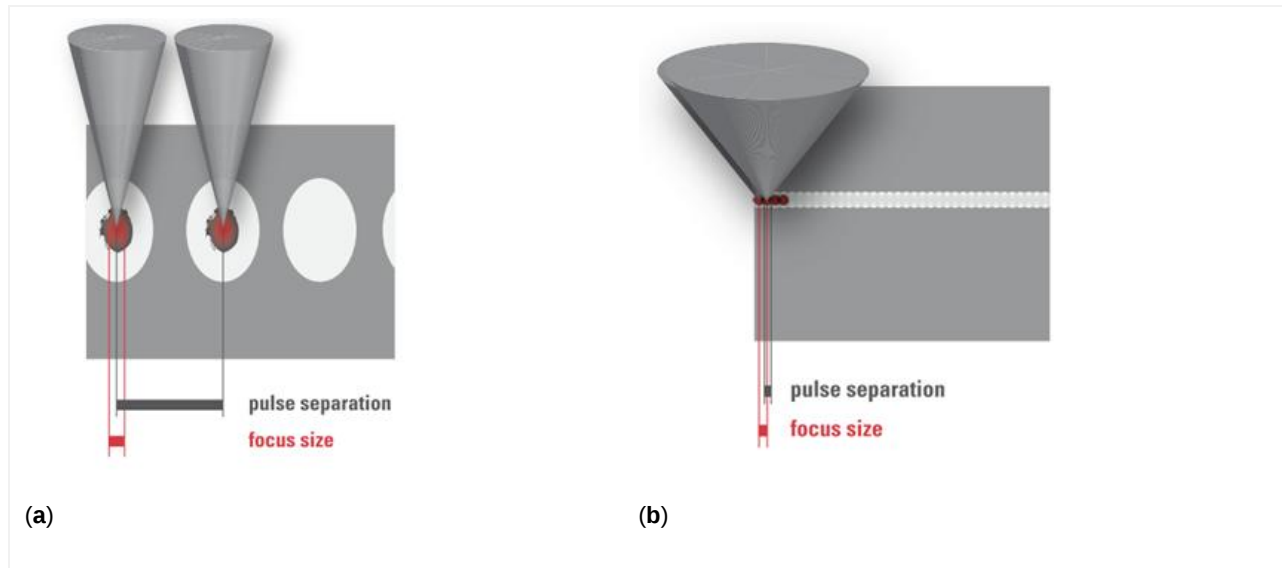

(**a**)   (**b**)

Figure 4. (**a**) High pulse energy, low repetition rate (large spot separation); (**b**) low pulse energy, high repetition rate (small spot separation, overlapping plasma effects of spots).

The cuts achieved by overlapping plasma evaporation of tissue by low energy pulses, however, have a uniquely smooth surface with virtually no damage to the adjacent tissue [19]. This is important for the quality of corneal "flaps", lenticules, or also smooth rims of capsulotomy cuts (see Sections 3.1.1, 3.1.2 and 3.3.2 below). High energy pulses with low repetition rate, on the other hand, rely on the mechanical tearing of tissue in between the actual laser foci. This tearing is accompanied by more stress or potentially even damage to the adjacent tissue [20], as shown by the levels of proinflammatory metabolics detected after laser treatments [21][22].

Software arranges the laser spots in the tissue into geometrical patterns. The software also uses scanning systems to position the laser foci in lines, planes, or even 3D geometries. An example of a 3D cut pattern used for cataract lens fragmentation (see Section 3.3.2 below), which combines multiple planes and cylinders, is shown in Figure 5.
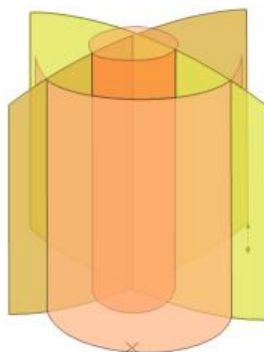

Figure 5. Three-dimensional laser focus scan pattern used for the fragmentation of cataractous lenses.

The energy of fs lasers with wavelengths in the 1030–1060 nm range is transmitted very well through all transparent structures of the eye. However, opaque material scatters the laser radiation and thus reduces the amount of energy reaching the laser focus. For example, laser cutting the cornea at locations with scars requires higher pulse energies than

in normal clear cornea. The energy losses depend on the thickness of the scattering material that the laser light is traveling through before reaching the focus. Therefore, the energy loss is more severe when cutting through a several mm thick nucleus of a cataractous lens than through corneal scars, which are only fractions of a mm thick.

The initial fs-laser systems designed for cataract surgery overcame this by using much higher pulse energies than fs lasers for cornea surgery. In the latest generation of versatile multipurpose ophthalmic fs-laser systems, the pulse energy is adaptable over an extensive range, so that for each situation, the adapted amount of pulse energy can be used, but not more, to minimize side effects, such as excessive gas production.

2.3. Supporting Technology Needed in Ophthalmic Fs-Laser Systems

To make an fs-laser device practical for clinical use, some critical supporting technologies needed to be developed as well. Most notable is optical coherence tomography (OCT) imaging of tissue structures, required for the precise positioning of laser cuts deep inside the eye, and the patient interface system using sterile vacuum docking methods to reliably connect the eye to the optical laser delivery system during treatment.

2.3.1. OCT Imaging

OCT is an optical technology that allows for scanning structures inside tissues, thus generating images [23][24]. The images appear similar to ultrasound images but with higher resolution.

The first application of OCT for biological purposes was described by Adolf Fercher et al. for the in vitro measurement of the axial eye length in 1988 (FERCHER 1988). The early clinical OCT systems used so-called time-domain (TD) OCT technology, where the length of the reference arm of an interferometer is mechanically changed. Due to speed limits of this process, these early devices were limited to one-dimensional scans (A-scans), or later small time consuming 2D scans. The so-called frequency-domain OCT (FD-OCT) technology meant a technological breakthrough—it used a fixed reference arm length but a spectrometer with a linear detector array instead of a single detector. Optical path length differences between the interferometer arms in this case produce a periodic modulation in the interference spectrum. By Fourier transformation, an entire A-scan can be retrieved from the measured spectrum [2] FD-OCT enabled much higher scan speeds, making 2D-imaging and even 3D-imaging feasible in clinical ophthalmology. The first ophthalmic application of FD-OCT, also known as "Fourier domain", was published in 2002 [25].

Later, a further improved variation of frequency-domain OCT technology was developed, "swept-source" (SS) OCT. In this case, a tunable light source with a frequency sweep indicated by a "sawtooth" frequency profile over time is used in combination with a fast single-pixel detector instead of a spectrometer. For further details of OCT technology, and advantages and limitations of its different versions, Section 7.3 of the textbook by Kaschke et al. [2] provides a comprehensive overview and additional literature references.

The initial ophthalmic use of OCT was exclusively for retinal imaging. Starting in 1994, the technology was also developed for imaging the anterior segment of the eye [26]. The possibility of quickly creating high-resolution cross-section images of the cornea, anterior chamber, and lens was a prerequisite for practical cataract surgery laser systems. Imaging and OCT guided surgery was first envisioned by Zeiss and first demonstrated for femtosecond laser surgery by H. Lubatschowski et al. [27].

In most modern cataract fs-laser systems, three-dimensional OCT scans are performed after docking the laser interface to the eye. The LensAR system uses a different technology, a proprietary 3D confocal structured illumination combined with Scheimpflug imaging [28]. In both cases, the resulting images are then analyzed by image processing software, identifying the tissue boundaries of interest [29]. These are notably the anterior and posterior sides of the cornea, the anterior and posterior surfaces of the lens, and the iris (see Figure 6).

This information is used to automatically propose the suitable positions inside the eye for the planned laser cuts, which are also displayed on screens for checking and confirmation by the eye surgeon (Figure 6).
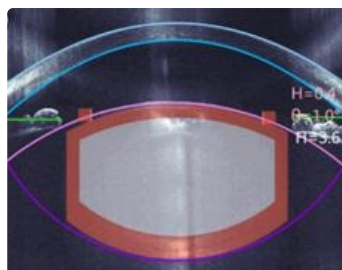
Figure 6. Example of the optical coherence tomography (OCT)-guided placement of an fs-laser cut pattern (blue: corneal anterior and posterior surface; pink and purple: lens anterior and posterior surface; green: iris plane).

2.3.2. Vacuum Docking Interfaces

For some laser systems, the patient's head is placed under a gantry containing focusing optics at a sufficiently long distance to allow the patient's head to move in and out. In other systems, an articulated arm with a handpiece with focusing optics at its end is used. Due to the flexible arm, the optics can be moved very close to the eye (Figure 7).
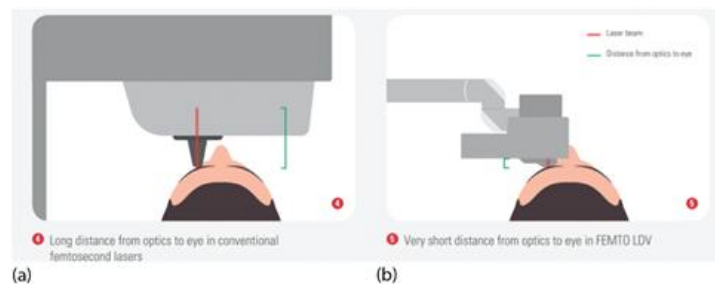

Figure 7. Typical eye docking methods of fs lasers: (**a**) head under fixed laser housing, (**b**) articulated arm with handpiece placed onto the eye; green: distance of eye surface to laser optics.

The eye's actual contact is established via sterile, single-use parts, so-called "patient interfaces". Two different types are in use: (a) applanating interface with a curved or flat interface directly touching the cornea, and (b) liquid-filled interface, where a vacuum ring creates contact to the sclera or the outer cornea, and the center is filled with liquid. The liquid-filled interface allows laser energy transmission while leaving the cornea in its natural shape (Figure 8) [30]. Although contact interfaces temporarily change the shape of the cornea [31], the mechanical contact stabilizes the cornea during surgery to a high degree. This is of particular importance in refractive surgery where precise cuts are required and tissue displacement on a micrometer level has to be avoided. With the absence of clear clinical drawbacks in refractive surgery [32][33][34], contact interfaces will play a dominant role in the future in corneal surgery. Liquid-filled interfaces with little disturbance of the eye might turn out to be the preferred solution in cataract surgery.
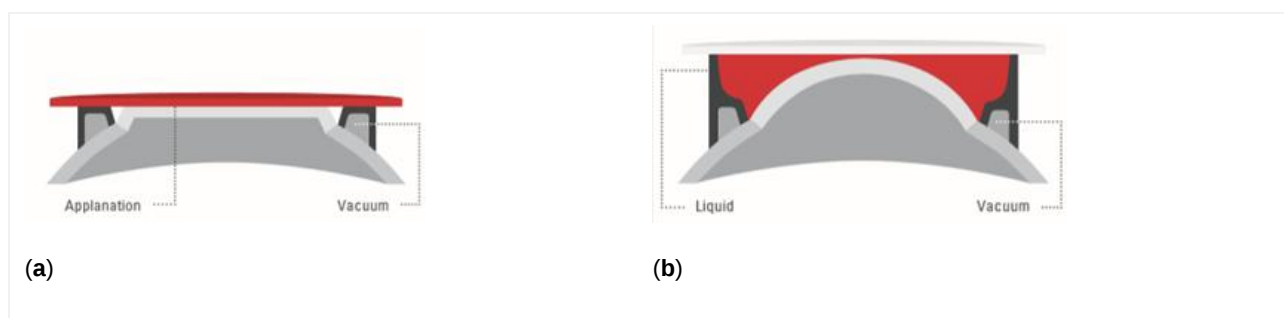

(**a**)   (**b**)

Figure 8. Typical patient interface designs: (**a**) contact interface in direct touch with the cornea (flat or curved), and (**b**) liquid optics interface, no direct touch on the cornea, no deformation.

The stability of the vacuum docking contact during laser emission is of primordial importance. Loss of contact harbors the risk of cutting in wrong planes. Therefore, all lasers are designed to automatically monitor vacuum levels, sometimes complemented with imaging of the eye position (eye tracking), and to immediately stop laser emission upon loss of contact. Of course, the eye surgeons also monitor their patients during the procedure and can manually interrupt or temporarily pause the treatment when they anticipate problems. In case of laser systems with an articulated arm, the surgeons can also use their substantial manual skills to actively stabilize the laser handpiece while in contact with the eye. In any case, after a vacuum loss, the treatment can usually be resumed immediately after a new docking.

References

1. Welch, A.J.; van Gemert, M. Optical-Thermal Response of Laser-Irradiated Tissue; Springer: Berlin/Heidelberg, Germany, 2011.

2. Kaschke, M.; Donnerhacke, K.-H.; Rill, M.S. Optical Devices in Ophthalmology and Optometry: Technology, Design Principles and Clinical Applications; WILEY-VCH Verlag GmbH & Co. KGaA: Weinheim, Germany, 2014.

3. Aron-Rosa, D.; Aron, J.J.; Griesemann, M.; Thyzel, R. Use of the neodymium-yag laser to open the posterior capsule after lens implant surgery: A preliminary report. Am. Intra-Ocular Implant. Soc. J. 1980, 6, 352–354, doi:10.1016/s0146-2

776(80)80036-x.

4. Stern, D.; Schoenlein, R.W.; Puliafito, C.A.; Dobi, E.T.; Birngruber, R.; Fujimoto, J.G. Corneal Ablation by Nanosecond, Picosecond, and Femtosecond Lasers at 532 and 625 nm. Arch. Ophthalmol. 1989, 107, 587–592, doi:10.1001/archopht.1989.01070010601038.

5. Huang, D.; Swanson, E.A.; Lin, C.P.; Schuman, J.S.; Stinson, W.G.; Chang, W.; Hee, M.R.; Flotte, T.; Gregory, K.; Puliafito, C.A.; et al. Optical Coherence Tomography. Science 1991, 254, 1178–1181.

6. Bhargava, R.; Kumar, P.; Phogat, H.; Chaudhary, K.P. Neodymium-yttrium aluminium garnet laser capsulotomy energy levels for posterior capsule opacification. J. Ophthalmic Vis. Res. 2015, 10, 37–42, doi:10.4103/2008-322x.156101.

7. Vogel, A.; Noack, J.; Hüttman, G.; Paltauf, G. Mechanisms of femtosecond laser nanosurgery of cells and tissues. Appl. Phys. A 2005, 81, 1015–1047, doi:10.1007/s00340-005-2036-6.

8. Heisterkamp, A.; Ripken, T.; Lubatschowski, H.; Welling, H.; Luetkefels, E.; Drommer, W.; Ertmer, W. Intrastromal cutting effects in rabbit cornea using femtosecond laser pulses. In Optical Biopsy and Tissue Optics; International Society for Optics and Photonics: Bellingham, WA, USA, 2000; pp. 52–60.

9. Pepose, J.S.; Lubatschowski, H. Comparing Femtosecond Lasers. Cataract Refract. Surg. Today 2008, 10, 45–51.

10. Vogel, A.; Busch, R. Shock Wave Emission and Cavitation Bubble Generation by Picosecond and Nanosecond Optical Breakdown in Water. J. Acoust. Soc. Am. 1996, 100, 148–165.

11. Vogel, A.; Venugopalan, V. Mechanisms of Pulsed Laser Ablation of Biological Tissues. Chem. Rev. 2003, 103, 577–644, doi:10.1021/cr010379n.

12. Tinne, N.; Knoop, G.; Kallweit, N.; Veith, S.; Bleeker, S.; Lubatschowski, H.; Krüger, A.; Ripken, T. Effects of cavitation bubble interaction with temporally separated fs-laser pulses. J. Biomed. Opt. 2014, 19, 48001, doi:10.1117/1.jbo.19.4.048001.

13. Lubatschowski, H.; Maatz, G.; Heisterkamp, A.; Hetzel, U.; Drommer, W.; Welling, H.; Ertmer, W. Application of ultrashort laser pulses for intrastromal refractive surgery. Graefe's Arch. Clin. Exp. Ophthalmol. 2000, 238, 33–39, doi:10.1007/s004170050006.

14. Ratkay-Traub, I.; Juhasz, T.; Horvath, C.; Suarez, C.; Kiss, K.; Ferincz, I.; Kurtz, R. Ultra-short pulse (femtosecond) laser surgery: Initial use in LASIK flap creation. Ophthalmol. Clin. N. Am. 2001, 14, 347–355.

15. Nagy, Z.Z.; McAlinden, C. Femtosecond laser cataract surgery. Eye Vis. 2015, 2, 1–8, doi:10.1186/s40662-015-0021-7.

16. Nagy, Z.; Takacs, A.; Filkorn, T.; Sarayba, M. Initial Clinical Evaluation of an Intraocular Femtosecond Laser in Cataract Surgery. J. Refract. Surg. 2009, 25, 1053–1060.

17. Ostovic, M.; Klaproth, O.K.; Hengerer, F.H.; Mayer, W.J.; Kohnen, T. Light Microscopy and Scanning Electron Microscopy Analysis of Rigid Curved Interface Femtosecond Laser-Assisted and Manual Anterior Capsulotomy. J. Cataract. Refract. Surg. 2013, 39, 1587–1592.

18. Lubatschowski, H. Overview of Commercially Available Femtosecond Lasers in Refractive Surgery. J. Refract. Surg. 2008, 24, S102–S107, doi:10.3928/1081597x-20080101-18.

19. Riau, A.K.; Liu, Y.C.; Lwin, N.C.; Ang, H.P.; Tan, N.Y.; Yam, G.H.; Tan, D.T.; Mehta, J.S. Comparative Study of Nj- and Muj-Energy Level Femtosecond Lasers: Evaluation of Flap Adhesion Strength, Stromal Bed Quality, and Tissue Responses. Invest. Ophthalmol. Vis. Sci. 2014, 55, 3186–3194.

20. Mayer, W.J.; Klaproth, O.K.; Ostovic, M.; Terfort, A.; Vavaleskou, T.; Hengerer, F.H.; Kohnen, T. Cell Death and Ultrastructural Morphology of Femtosecond Laser–Assisted Anterior Capsulotomy. Investig. Opthalmology Vis. Sci. 2014, 55, 893–898, doi:10.1167/iovs.13-13343.

21. Schultz, T.; Joachim, S.C.; Stellbogen, M.; Dick, H.B. Prostaglandin Release During Femtosecond Laser-Assisted Cataract Surgery: Main Inducer. J. Refract. Surg. 2015, 31, 78–81, doi:10.3928/1081597x-20150122-01.

22. Schwarzenbacher, L.; Schartmueller, D.; Leydolt, C.; Menapace, R. Intra-individual comparison of cytokine and prostaglandin levels with and without low-energy, high-frequency femtosecond laser cataract pretreatment following single-dose topical NSAID application. J. Cataract. Refract. Surg. 2020, 46, 1086–1091, doi:10.1097/j.jcrs.0000000000000221.

23. Fercher, A.F.; Drexler, W.; Hitzenberger, C.K.; Lasser, T. Optical Coherence Tomography—Principles and Applications. Rep. Prog. Phys. 2003, 66, 239–303.

24. Schuman, J.S.; Puliafito, C.A.; Fujimoto, J.G.; Duker J.S. Optical Coherence Tomography of Ocular Diseases; Slack Inc.: San Francisco, CA, USA, 2012.

25. Wojtkowski, M.; Leitgeb, R.A.; Kowalczyk, A.; Bajraszewski, T.; Fercher, A.F. In vivo human retinal imaging by Fourier domain optical coherence tomography. J. Biomed. Opt. 2002, 7, 457–463, doi:10.1117/1.1482379.

26. Izatt, J.A.; Hee, M.R.; Swanson, E.A.; Lin, C.P.; Huang, D.; Schuman, J.S.; Puliafito, C.A.; Fujimoto, J.G. Micrometer-Scale Resolution Imaging of the Anterior Eye in Vivo with Optical Coherence Tomography. Arch. Ophthalmol. 1994, 112, 1584–1589.

27. Kermani, O.; Fabian, W.; Lubatschowski, H. Real-Time Optical Coherence Tomography-Guided Femtosecond Laser Sub-Bowman Keratomileusis on Human Donor Eyes. Am. J. Ophthalmol. 2008, 146, 42–45, doi:10.1016/j.ajo.2008.03.003.

28. Chang, J.S., Chen, I.N., Chan, W.M., Ng, J.C., Chan, V.K. Law AK. Initial evaluation of a femtosecond laser system in cataract surgery. J Cataract Refract Surg. 2014, 40, 29–36. doi: 10.1016/j.jcrs.2013.08.045.

29. Grewal, D.S.; Schultz, T.; Basti, S.; Dick, H.B. Femtosecond laser–assisted cataract surgery—Current status and future directions. Surv. Ophthalmol. 2016, 61, 103–131, doi:10.1016/j.survophthal.2015.09.002.

30. Talamo, J.H.; Gooding, P.; Angeley, D.; Culbertson, W.W.; Schuele, G.; Andersen, D.; Marcellino, G.; Essock-Burns, E.; Batlle, J.; Feliz, R.; et al. Optical patient interface in femtosecond laser–assisted cataract surgery: Contact corneal applanation versus liquid immersion. J. Cataract. Refract. Surg. 2013, 39, 501–510, doi:10.1016/j.jcrs.2013.01.021.

31. Mirshahi, A.; Kohnen, T. Effect of Microkeratome Suction During LASIK on Ocular Structures. Ophthalmology 2005, 112, 645–649, doi:10.1016/j.ophtha.2004.11.046.

32. Flaxel, C.J.; Choi, Y.H.; Sheety, M.; Oeinck, S.C.; Lee, J.Y.; McDonnell, P.J. Proposed Mechanism for Retinal Tears after Lasik: An Experimental Model. Ophthalmology 2004, 111, 24–27.

33. Kanclerz, P.; Grzybowski, A. Does Corneal Refractive Surgery Increase the Risk of Retinal Detachment? A Literature Review and Statistical Analysis. J. Refract. Surg. 2019, 35, 517–524, doi:10.3928/1081597X-20190710-02.

34. Toth, C.A.; Mostafavi, R.; Fekrat, S.; Kim, T. LASIK and vitreous pathology after LASIK. Ophthalmology 2002, 109, 624–625, doi:10.1016/s0161-6420(02)00996-x.